Analyst

Image analysis for a microfluidic paper-based analytical device using the CIE *L*a*b** color system†

Takeshi Komatsu,[a] Saeed Mohammadi,[a] Lori Shayne Alamo Busa,‡[a]
Masatoshi Maeki,[b] Akihiko Ishida,*[b] Hirofumi Tani[b] and Manabu Tokeshi*[b,c,d,e]

The combination of a microfluidic paper-based analytical device (μPAD) and digital image analysis is widely used for quantitative analysis with μPADs because of its easy and simple operation. Herein, we have demonstrated a quantitative analysis based on multiple color changes on a μPAD. The CIE *L*a*b** color system was employed to analyse the digital images obtained with the μPAD. We made pH measurements using a universal pH-indicator showing multiple color changes for various pH values of aqueous test solutions. The detectable pH range of this method was wider than the typical grayscale-based image analysis, and we succeeded in the measurements for a wide pH range of 2–9.

Since the first report of a μPAD in 2007 by Whitesides's group as an inexpensive analytical and diagnostic device,[1] μPADs have steadily gained attention and interest among researchers.[2–4] The μPADs have a great potential as analytical devices in resource-limited settings because they are inexpensive, easy-to-use and require no special measuring instruments. Several types of fabrication methods have been developed including photolithography,[5,6] screen printing,[7] wax printing,[8,9] inkjet printing[10,11] and cutting.[12] Several detection methods for the μPADs have also been proposed such as colorimetric,[1,6] fluorescence,[13] electrochemical,[7] and electrochemiluminescence[14] methods. In these detection methods,

colorimetric methods based on an image analysis of digital images of the device are most widely used because they are simple and easy-to-use. These methods require no special apparatus, only a digital camera or a smartphone, and allow quantitative analysis by reading out the color information (RGB value or CMYK value) of the detection area of a μPAD in the digital image. The color information is mainly obtained as separate RGB channel values or grayscale, which give the amount of analyte on the basis of the relationship between the color information and the analyte concentration. Several software applications for smartphones have been developed to perform image analysis of the μPAD images.[15,16] Therefore, a combination of μPADs and image analysis is a suitable technique for point of care testing and applications in resource-limited settings. The grayscale (the average of RGB values) is one of the most common measure in image-analysis based colorimetry.[6,17–19] However, the grayscale possibly does not allow quantitative analysis based on multiple changes of color such as a universal pH test strip because the grayscale cannot follow multiple color changes.

Herein, we report a simple colorimetric pH measurement method using a μPAD based on the CIE *L*a*b** color system. The CIE *L*a*b** color system has three coordinates L^*, a^*, and b^*. The L^* value indicates lightness, and $(a^* + b^*)^{1/2}$ and $\tan^{-1}(b^*/a^*)$ indicate chroma (C_{ab}) and hue angle (h_{ab}), respectively. The color difference (ΔE) between an objective color and a reference one is given by the following equation:[20–22]

$$\Delta E = \sqrt{(a_x - a_0)^2 + (b_x - b_0)^2 + (L_x - L_0)^2} \qquad (1)$$

where subscripts x and 0 denote objective and reference, respectively. Abe *et al.*[11] previously demonstrated the pH measurement using a universal pH indicator and the a^* coordinate. However, the reported method did not cover a wide pH range because of lack of color information. The a^* coordinate indicates redness and greenness for the positive ($+a^*$) and negative ($-a^*$) direction, respectively. The a^* value is given by $a^* = C_{ab} \times \cos(h_{ab})$. The colors (red and orange) appearing at low pH values (see Fig. 1) correspond to small hue angles. This

[a] Graduate School of Chemical Sciences and Engineering, Hokkaido University, Kita 13 Nishi8, Kita-ku, Sapporo 060-8628, Japan

[b] Division of Applied Chemistry, Faculty of Engineering, Hokkaido University, Kita 13 Nishi 8, Kita-ku, Sapporo 060-8628, Japan.
E-mail: ishida-a@eng.hokudai.ac.jp; Fax: +81-11-706-6745; Tel: +81-11-706-6746

[c] ImPACT Research Centre for Advanced Nanobiodevices, Nagoya University, Furo-cho Chikusa-ku, Nagoya 464-8603, Japan

[d] Innovative Research Centre for Preventive Medical Engineering, Nagoya University, Furo-cho Chikusa-ku, Nagoya 464-8603, Japan

[e] Institute of Innovation for Future Society, Nagoya University, Furo-cho, Chikusa-ku, Nagoya 464-8603, Japan. E-mail: tokeshi@eng.hokudai.ac.jp; Fax: +81-11-706-6745; Tel: +81-11-706-6744

†Electronic supplementary information (ESI) available. See DOI: 10.1039/c6an01409g

‡Present address: Natural Science Department, College of Arts and Sciences, Nueva Vizcaya State University, Bayombong, Nueva Vizcaya 3700 Philippines.
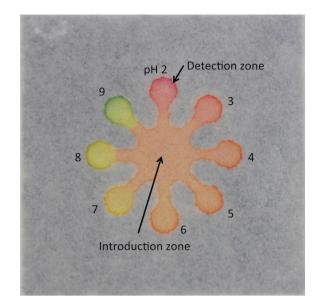
Fig. 1 Photograph of the μPAD producing multiple colors for various pH values (2–9). The μPAD had eight detection zones (φ = 4 mm) and an introduction zone (center part, φ = 12 mm). Aqueous solutions (0.5 μL) with different pH values were introduced into separate detection zones and the universal pH indicator (15 μL) was added to the introduction zone.

resulted in the small change in the $a*$ coordinate as shown in Fig. S3.† Thus, only the use of the $a*$ value is not suitable for pH measurement based on formation of multiple colors. Commonly, multiple-color changes have gained great attention in various assays, such as heavy metal assay[23] and enzymatic assay,[24,25] which could be applicable to μPAD formats. Therefore, we examined if the quantitative measurement of pH could be performed by using ΔE for multiple color changes because ΔE contains much color information.

We fabricated μPADs by the previously reported screen-printing method.[26] The μPAD had eight detection zones (diameter, 4 mm) and an introduction zone (diameter, 12 mm). The detection zones were connected to the introduction zone *via* microchannels (width = 2 mm). In brief, a piece of chromatography paper was fixed onto a printing table. A patterned screen stencil was placed onto the paper and the paper was kept in place on the printing table *via* a vacuum pump. Then, PDMS was poured onto the screen stencil, and a squeegee was used to rub the PDMS into the pattern openings. The PDMS-printed paper was cured in an oven at 120 °C for 30 min. The patterned paper was removed from the oven and cut into separate paper devices (30 × 30 mm).

In the pH measurement with the μPAD, 0.5 μL portions of aqueous solutions prepared at various pH values were introduced into the respective detection zones. After a 5 min incubation at room temperature, 15 μL of a universal pH indicator (the composition and the concentration are shown below and in the ESI†) was introduced into the introduction zone. After a 1 min incubation, a digital image of the μPAD was taken with a digital camera (EOS Kiss X6i, Canon, Tokyo, Japan) under fluorescent lighting conditions. The distance between

the μPAD and the camera was fixed to *ca.* 20 cm. The color information was obtained with an image analysis software program (ImageJ ver. 1.48).

To perform the pH measurement in a wide range of pH values, we used a universal pH indicator consisting of thymol blue (pK_{a_1} = 1.7, pK_{a_2} = 8.9; transition intervals, pH 1.2–2.8 and pH 7.8–9.5), methyl red (pK_a = 5.1, pH 4.2–6.2), bromothymol blue (pK_a = 7.1, pH 6.0–7.6), and phenolphthalein (pK_a = 9.3, pH 7.8–10.0).[9] Fig. 1 shows a photograph of the μPAD, showing that the pH indicator exhibited various colors, such as red, orange, yellow and green in response to the pH values of test solutions (pH 2–9) at the detection zones.

We analyzed the color of the detection zones in the digital images in the typical RGB color space and the CIE $L*a*b*$ color space. For the image analysis in the CIE $L*a*b*$ color space, the image was converted from the RGB color space to the CIE $L*a*b*$ color space with the Color Space Converter plugin in the image analysis software and then separated into respective channels of $L*$, $a*$, and $b*$. A circular region of interest (ROI, 27000 pixels) was selected around each detection zone and was analyzed using the software, as shown in Fig. S1† (a red dotted circle). The RGB values, grayscale, and respective $L*a*b*$ values of the selected region were obtained with the software. Each value was given as a mean in the region. Thus, the non-uniformity in the colors in each zone was flattened. Consequently, the non-uniformity had little effect on the assay results. We performed the assay in triplicate.

Fig. 2(a) shows plots of RGB values against the pH value. A plot of grayscale against the pH value was also prepared for reference (Fig. S2†). The RGB values and grayscale showed no monotonic change in response to the pH value of 2–9 and narrow detectable pH ranges with RGB values. This is due to the lack of color information because the respective RGB values show only the information of redness, greenness or blueness of the resulting colors. We also considered that large standard deviations were caused by the reproducibility of colors of the photograph. Therefore, the RGB value is not suitable for pH measurement in the μPAD giving multiple colors.

Next, the image analysis with the CIE $L*a*b*$ color coordinates ($L*$, $a*$, and $b*$) was performed. Fig. S3† indicates that the data points traced an arc, accompanying an increase in the pH value. Fig. S4† also shows dependencies of the pH value on each coordinate ($L*$, $a*$, and $b*$). The $a*$ value was decreased with increasing pH value. However, the $a*$ value shows no significant change at low pHs because of large standard deviation as shown in Fig. S4,† which suggests that the pH cannot be measured with the $a*$ value. The $b*$ value and the $L*$ value did not show monotonic changes in response to the pH value of 2–9 (Fig. S4†).

The color difference (ΔE) was calculated using eqn (1) with the values of L_0^*, a_0^*, and b_0^* for the color produced at pH 2. Fig. 2(b) shows that the ΔE value increased monotonously with increasing pH value with small standard deviations. This confirmed high assay reproducibility. The detectable pH range was wider than those obtained with the RGB-based image analysis and the single channel value of $L*$, $a*$, and $b*$. For com-
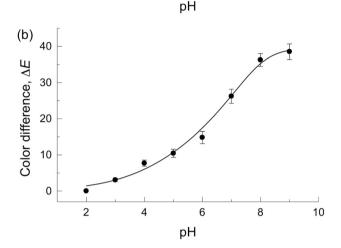
Fig. 2 Plots of (a) R, G, and B against pH value and (b) plot of CIE $L^*a^*b^*$ color difference against pH value. Data points represent the mean of 3 measurements and error bars represent one standard deviation from the mean. In panel (b), data were fitted to a sigmoidal curve ($R^2 = 0.982$).

parison, a $\tan^{-1}(b^*/a^*)$[15] vs. pH value plot was constructed (Fig. S5†) because $\tan^{-1}(b^*/a^*)$ contains the hue information as well as ΔE. The $\tan^{-1}(b^*/a^*)$ showed a linear relationship with the pH value in the range of 2–9 ($r^2 = 0.972$). However, the $\tan^{-1}(b^*/a^*)$ values showed larger standard deviation than ΔE at low pHs.

In conclusion, we demonstrated a simple pH measurement in the µPAD by a colorimetric method based on the CIE $L^*a^*b^*$ color difference (ΔE). The use of ΔE was suitable for a colorimetric pH measurement based on the multiple color changes due to the universal pH indicator. We expect that the combination of the µPAD and image analysis based on color difference ΔE will enable quantitative analysis for multiple color changes.[24] The present paper-based analytical method will accelerate applications to point of care testing and in resource-limited settings.

Acknowledgements

References

1 A. W. Martinez, S. T. Philips, M. J. Butte and G. M. Whitesides, *Angew. Chem., Int. Ed.*, 2007, **46**, 1318–1320.

2 D. M. Cate, J. A. Adkins, J. Mettakoonpitak and C. S. Henry, *Anal. Chem.*, 2015, **87**, 19–41.

3 Y. Xia, J. Si and Z. Li, *Biosens. Bioelectron.*, 2016, **77**, 774–789.

4 L. S. A. Busa, S. Mohammadi, M. Maeki, A. Ishida, H. Tani and M. Tokeshi, *Micromachines*, 2016, **7**, 86.

5 A. W. Martinez, S. T. Phillips, G. M. Whitesides and E. Carrilho, *Anal. Chem.*, 2010, **82**, 3–10.

6 A. W. Martinez, S. T. Phillips, E. Carrilho, S. W. Thomas III, H. Sindi and G. M. Whitesides, *Anal. Chem.*, 2008, **80**, 3699–3707.

7 W. Dungchai, O. Chailapakul and C. S. Henry, *Anal. Chem.*, 2009, **81**, 5821–5826.

8 E. Carrilho, A. W. Martinez and G. M. Whitesides, *Anal. Chem.*, 2009, **81**, 7091–7095.

9 S. Karita and T. Kaneta, *Anal. Chem.*, 2014, **86**, 12108–12114.

10 K. Yamada, T. G. Henares, K. Suzuki and D. Citterio, *Angew. Chem., Int. Ed.*, 2015, **54**, 5294–5310.

11 K. Abe, K. Suzuki and D. Citterio, *Anal. Chem.*, 2008, **80**, 6928–6934.

12 W. Liu, Y. Guo, M. Zhao, H. Li and Z. Zhang, *Anal. Chem.*, 2015, **87**, 7951–7957.

13 N. K. Thom, G. G. Lewis, K. Yeung and C. T. Phillips, *RSC Adv.*, 2014, **4**, 1334–1340.

14 N. Hao, M. Xiong, J. D. Zhang, J. J. Xu and H. Y. Chen, *Anal. Chem.*, 2013, **85**, 11715–11719.

15 N. Lopez-Ruiz, V. F. Curto, M. M. Erenas, F. Benito-Lopez, D. Diamond, A. J. Palma and F. Capitan-Vallvey, *Anal. Chem.*, 2014, **86**, 9554–9562.

16 C. Sicard, C. Glen, B. Aubie, D. Wallace, S. Jahanshahi-Anbuhi, K. Pennings, G. T. Daigger, R. Pelton, J. D. Brennan and C. D. M. Filipe, *Water Res.*, 2015, **70**, 360–369.

17 S. J. Vella, P. Beattie, R. Cademartiri, A. Laromaine, A. W. Martinez, S. T. Phillips, K. A. Mirica and G. M. Whitesides, *Anal. Chem.*, 2012, **84**, 2883–2891.

18 X. Mu, L. Zhang, S. Chang, W. Cui and Z. Zheng, *Anal. Chem.*, 2014, **86**, 5338–5344.

19 L. Cai, Y. Wang, Y. Wu, C. Xu, M. Zhong, H. Lai and J. Huang, *Analyst*, 2014, **139**, 4593–4598.

20 E. Hirayama, T. Sugiyama, H. Hisamoto and K. Suzuki, *Anal. Chem.*, 2000, **72**, 465–474.

21 M. Maskan, *J. Food Eng.*, 2001, **48**, 169–175.

22 R. S. Berns, *Billmeyer and Saltzman's Principles of Color Technology*, John Wiley & Sons, 3rd edn, 2000.

23 D. Li, X. Sun, M. Wang, H. Yu, H. Zhou, J. Wu and Y. Tian, *Sens. Actuators, B*, 2015, **220**, 1006–1016.

24 A. Ishida, Y. Yamada and T. Kamidate, *Anal. Bioanal. Chem.*, 2008, **392**, 987–994.

25 C. Li, Y. Yang, D. Wu, T. Li, Y. Yin and G. Li, *Chem. Sci.*, 2016, **7**, 3011–3016.

26 S. Mohammadi, M. Maeki, R. M. Mohamadi, A. Ishida, H. Tani and M. Tokeshi, *Analyst*, 2015, **140**, 6493–6499.